

Measuring entropy generated by spin-transfer

J.-E. Wegrowe* and Q. Anh Nguyen, T.L. Wade

Laboratoire des Solides Irradiés, Ecole Polytechnique, 91128 Palaiseau Cedex, France.

(Dated: December 6, 2018)

Abstract

An experimental protocol is presented that allows the entropy generated by spin-transfer to be measured. The effect of a strong spin-polarized current injected on a ferromagnetic nanostructure is investigated with focusing on the quasi-static equilibrium states of a ferromagnetic single domain. The samples are single contacted Ni nanowires obtained by electrodeposition in a nanoporous template. The thermal susceptibility of the magnetoresistance is measured as a function of the magnetic field for different values of the current injected through the wire. This quantity is related to the thermal magnetic susceptibility of the ferromagnetic wire through the anisotropic magnetoresistance. The ferromagnetic entropy generated by the current injection is deduced thanks to a thermodynamic Maxwell relation. This study shows that the effect of the spin-transfer in our samples results in the generation of incoherent excitations instead of rotation of the magnetization.

PACS numbers: 75.40.Gb, 72.25.Hg, 75.47.De

*Electronic address: jean-eric.wegrowe@polytechnique.edu

Spin-transfer is the generic name for the effect of magnetization reversal or magnetic excitations produced by the injection of a spin-polarized current in a ferromagnetic nanostructure. Since the discovery of spin-transfer effects in various kinds of systems [1], some fundamental questions emerged about the stochastic vs. deterministic nature of the effect. Already in the pioneering theoretical works about spin-transfer, the two approaches were suggested. Luc Berger [2] proposed first a non-deterministic approach with calculating an electronic s-d mean relaxation time that defines the transfer of spins from the electric current to the lattice (a consequence of which is to generate spin-waves). On the other hand, Slonczewski proposed a determinist term to be added to the Landau-Lifshitz-Gilbert equation of the dynamics of the ferromagnet [3] (this term is the expression of a torque exerted on the ferromagnet). The deterministic term is of "dissipative" nature, however, in the case of homogeneous magnetization, the corresponding effective fields still derive from two deterministic potentials [4, 5]. The two approaches are actually difficult to discriminate because the deterministic terms may also justify the existence of incoherent excitations, which eventually lead to the magnetization reversal.

In the years that followed this discovery, many different aspects of spin-transfer have been investigated experimentally, especially in terms of critical currents necessary to switch the magnetization (at a given excitation time scale). However, the important point that motivated this work is that the measure of the critical current is a measure of the magnetic relaxation, so that it involves the stochastic process describe by the Néel-Brown activation [4]. The consequence is that the process measured by the critical current is stochastic, whatever the nature of the underlying mechanism, and after ten years of spin-transfer measurements it is still difficult to understand the very nature of the underlying magnetic process. Should spin-transfer be described by a deterministic expression in the ferromagnetic dynamic equation, or should spin-transfer be described by diffusion or fluctuations in the corresponding stochastic equation? Or even more basically: does spin-transfer produce coherent rotation or precession of the magnetization (without the help of an external AC excitation), or incoherent excitations? The ambition of this work is to answer these questions.

It is worth pointing out that despite an intense research activity on this topic, the simplest experiments that would avoid the activation process, namely measuring the rotation of the magnetization due to current injection on the *quasi-static equilibrium states*, i.e. measuring the modification of the reversible part of the hysteresis loop, has not been reported as such.

This situation is rather surprising since it would be the most direct way to obtain the deterministic terms predicted by Slonczewski and to exhibit the corresponding potentials.

One problem of the quasi-static measurements is due to the difficulty of measuring precisely the magnetization states of individual single ferromagnetic domains (contacted to a current source) as a function of the electric current densities, for very high densities injected. Adding to the difficulty of measuring the magnetization states at the nanoscale, many collateral effects of thermodynamic nature take place. Joule heating is of course superimposed on the effect of the spin-polarized current injection, but also induce fields and some important thermoelectric effects [6].

The aim of this paper is to present a new experimental protocol that allows the effect of spin-injection to be investigated on the quasi-static states of the magnetization, to present the results obtained, and to discuss the results in terms of ferromagnetic fluctuations generated by spin-transfer. This goal is achieved thanks to remarkable thermodynamic properties of ferromagnets. In analogy with magnetocaloric effects, we show that thermal susceptibility measurements of the anisotropic magnetoresistance of a single ferromagnetic domain give access to the entropy production, and that this method furnishes a sensitive probe of the ferromagnetic fluctuations generated by spin-injection (i.e. spin-transfer). It is interesting to recall that such an approach was used for the first experimental evidence of the spontaneous magnetization of a ferromagnet as well as the first check of the mean field theory [7].

The structure used for this investigation is a single contacted Ni nanowire, obtained by electrodeposition into nanoporous polycarbonate membranes. This sample is chosen for convenience as typical test system thanks to previous studies related to the magnetization states [8, 9, 10, 11], to spin-transfer measured for the irreversible jumps of the magnetization [12, 13, 14, 15], and spin-dependent thermoelectric power [16, 17, 18, 19]. The nanowire can be described as a single ferromagnetic layer with two ferromagnetic/normal interfaces [4]. The magnetization is uniform for all equilibrium states: $\vec{M} = M_s \cdot \vec{u}_r$, where M_s is the magnetization at saturation, and \vec{u}_r is the radial unit vector. In contrast to the spin-valve systems, the ferromagnetic layer is large with respect to the spin-diffusion length (and to other typical relaxation lengths), i.e. large with respect to the interfaces. This system is simple enough to discriminate easily between bulk and interface effects, which is the very first step in the understanding of the measured effects (see references [17, 18]). The protocol described here can also be applied as such on typical pillar spin-valves and

tunneling junctions, e.g. the memory units used for Magnetic Random Access Memory (MRAM) applications.

For nanowires composed by a uniform ferromagnetic layer, the magnetization is measured through the anisotropic magnetoresistance (AMR). The giant magnetoresistance (GMR) cannot be measured directly with one magnetic layer because there is no reference states for spin-flip scattering [4]. Nevertheless, spin-accumulation (responsible for the GMR in spin-valve structures) is present at the interfaces between the normal metal and the Ni in both sides of the wire [18], and spin-transfer is clearly observed [12, 13, 14, 15, 20, 21].

The experimental protocol adopted here in order to access to the effect of spin transfer on the reversible part of the hysteresis is the following: the thermal susceptibility of the magnetization $\chi_T = \frac{1}{M_s} \frac{\partial M}{\partial T}$ (where T is the temperature of the wire and M_s its magnetization at saturation) is measured through the variation of the AMR in phase with the temperature. The measurements are performed as a function of the external field, and as a function of the amplitude of the current injected.

The field dependent thermal susceptibility allows the ferromagnetic entropy production to be obtained, according to the Maxwell relation: $(\frac{\partial S}{\partial H})_T = (\frac{\partial M}{\partial T})_H$. The validity of the Maxwell relation is assumed because the total magnetic system is considered (a closed ferromagnetic system that takes into account the spin-dependent current generator and the ferromagnetic layer is defined in the references [4, 22]), and because only the reversible part of the magnetization curve is taken into account (see [23] otherwise).

The paper is composed as follows: the first part is devoted to the characterization of the ferromagnetic states, with the use of the AMR properties of the Ni nanowires. The second part presents the measurement protocol and the relations that link the measured thermal susceptibility to the fluctuations and to the usual field susceptibility $\chi_H = \frac{1}{M_s} \frac{\partial M}{\partial T}$ deduced from the AMR. The third part shows the action of high current densities on this susceptibility and the entropy generated by spin-transfer. We conclude that the effect of the spin-transfer in our samples results in the generation of incoherent excitations.

A. AMR and the reversible part of the hysteresis

The interest in working with Ni nanowires is that the ferromagnetic states are well known and are easy to describe [9, 10, 11, 14]. The wires length is $l = 6 \mu\text{m}$ and the diameters

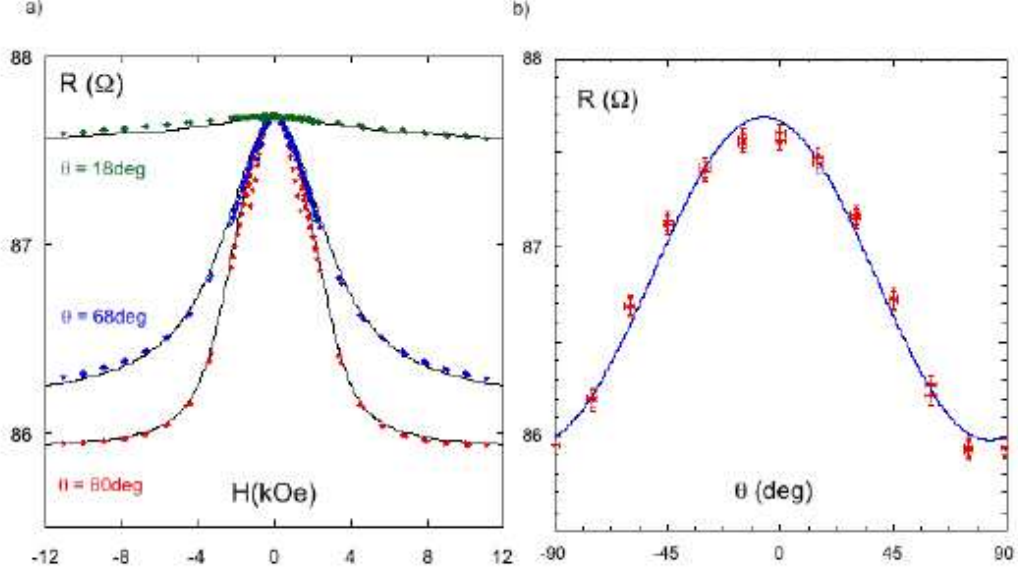


FIG. 1: (a) AMR hysteresis loops as a function of the external field for different angles with respect to the wire axis (dots). The lines represent the reversible part of the hysteresis calculated for a uniform and uniaxial Ni nanowire (using the potential Eq. (2) and the magnetoresistance Eq. (1)) for the angles 18° , 69° and 80° . (b) AMR as a function of the angle of the magnetization at saturation field. The continuous line is the $\cos^2(\theta)$ of curve of Eq. (1).

is about 60 nm (aspect ratio 100). The electrodeposited Ni is composed of very small crystallites inside the wire, so that the magnetocrystalline anisotropy is averaged-out over some tens of nanometers. From the ferromagnetic point of view the anisotropy is uniaxial, because it is reduced to the shape anisotropy of a very long cylinder (with aspect ratio 100, the demagnetizing factor is very close to that of an infinite cylinder).

The wires are contacted individually by an in-situ method inside the electrolytic bath. The method consists in depositing a thin gold layer on the top of the membrane (without obstruction of the pores) in order to measure the potential between the top and the bottom of the membrane during the growth of Ni. A feed-back loop allows the deposition to be stop for a single wire contacted [24]. The fabrication process is described elsewhere [25]. The wire is contacted to a current source and a voltmeter.

The resistance hysteresis loops, measured as a function of the amplitude of the magnetic field and for different field directions, are plotted in Fig. 1 (a). Fig. 1 (b) shows the AMR

measured at saturation field ($H = 1.2T$) and plotted as a function of the field direction (defined by the angle θ). At saturation field, the direction of the field \vec{H} coincides with the direction of the magnetization \vec{M} (defined by the angle φ in the following) so that $\theta = \varphi$. Furthermore, in the case of the nanowire, the angle φ is also the angle between the current density \vec{J} (oriented along the wire axis) and the magnetization $\varphi = (\vec{J}, \vec{M})$. The Fit in Fig. 1(b) shows that $R(\varphi) = R(\varphi = 90^\circ) + (R(\varphi = 0) - R(\varphi = 90^\circ)) \cos^2(\varphi)$. The magnetoresistance is hence reduced to the AMR contribution only [26].

As expected for a single domain ferromagnetic layer, the profile plotted in Fig. 1(a) is composed of four reversible parts of the hysteresis and two symmetric irreversible jumps joining the reversible branches. The succession of quasi-static states that defines each branch of the hysteresis is indeed reversible.

Thanks to the wire's geometry, the maximum of the resistivity ρ_{\parallel} corresponds to the magnetization parallel to the wire axis ($\theta = 0$) while the minimum corresponds to the magnetization perpendicular to the wire axis ρ_{\perp} . The uniform rotation of the magnetization, $\cos(\varphi(H)) = M(H)/M_s$ leads to the simple expression that relates the magnetoresistance hysteresis loop to the magnetic hysteresis loop [9]:

$$\rho(H, T) = \rho_{\perp}(T) + \Delta\rho(T) \left[\frac{M(H, T)}{M_s} \right]^2 \quad (1)$$

where $\Delta\rho = \rho_{\parallel} - \rho_{\perp}$, and the measured hysteresis $M(H)$ is that obtained by projection over the wire axis.

On the other hand, the quasi-static states of the magnetization, that defines the reversible part of the hysteresis loop, are given by the equilibrium condition $\partial V / \partial \vec{M} = 0$ [27]. In the case of the Ni nanowires, the magnetization states at equilibrium are uniform, and the anisotropy, reduced to the shape anisotropy, is uniaxial. The Gibbs energy of the Ni nanowire writes :

$$V(\varphi, H) = K \sin^2(\varphi) - M_s H \cos(\theta - \varphi) \quad (2)$$

where H is the amplitude of the magnetic field applied at an angle θ and φ is the angle of the magnetization with respect to the wire axis. Introducing Eq. (2) into the equilibrium conditions gives the reversible part of the hysteresis:

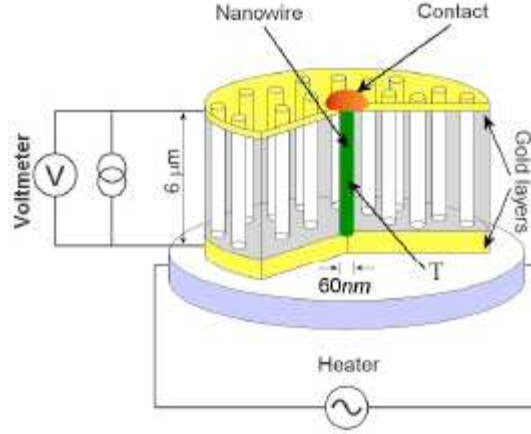


FIG. 2: Schematic of the membrane with the contacted nanowire and the heater.

$$K \sin(2\varphi) - M_s H \sin(\theta - \varphi) = 0 \quad (3)$$

The curves plotted in Fig. 1(a), calculated for the three angles 18° , 68° , and 80° , are obtained by using Eq. (3) including the AMR formula (1) (a first fit is performed at 80° for adjusting the resistance and the anisotropy parameter K , and the other curves are deduced without adjusting parameters; the parameter K is that used in the curve plotted in Fig. 1(b)). The validity of this description is confirmed by the calculated curves Fig. 1(a) and Fig. 1(b). The anisotropy field is found to be $H_a = 3 kOe$. This is the value expected for the anisotropy field of an infinite cylinder $H_a = \mu_0 M_s / 2 = 3,05 kOe$.

B. Measure of the thermal susceptibility

In order to measure the thermal susceptibility, a Joule heater is fixed on the bottom of the membrane (see Fig. 2). The membrane is hence composed of the heater on the bottom with a 250 nm gold layer, and a submicrometric Ni mushroom that forms the contact on the surface of the second gold layer of about 50 nm thickness.

The analysis of the heat conductivity regimes inside the wire [13] shows that the temperature of the membrane is not significantly modified, and the heat propagates from the bottom layer to the top layer through the contacted wire.

The experimental protocol established in order to measure the thermal susceptibility is as

follows. A sinusoidal temperature variation is imposed on the wire through the heater and the response of the voltage (i.e. the magnetoresistance) is measured in phase. The heater is controlled by a heat current oscillating at frequency f , $I_{heat} = I_{h0} \cos(2\pi f)$, where I_{h0} is of the order of 1 mA. The heat power is dispersed into the whole structure, and only a small but sufficient fraction of the power is used to heat the wire. The temperature inside the wire is measured precisely with the resistance of the wire itself (typically, the resistivity is of the order of $5 \cdot 10^{-8} \Omega \cdot m$ and the variation due to the heater is about 1 %). The corresponding temperature variation ΔT of the wire is of the order of 3 degrees around the temperature $T_0 \approx 300 K$. At stationary regime, the mean temperature of the wire follows the heater, and oscillates in time at the frequency $2f$. In order to reach a well defined thermal stationary regime, the frequency of the signal is fixed at $f = 0.05 Hz$. The duration of each measurement is of the order of 120 sec. Since the wire reaches its thermal equilibrium much more rapidly [13], each measured point is isothermic. This protocol is necessary in order to extract the response of the system to the thermal excitation, with the exclusion of the other contributions: drifts, thermal instabilities, electromigration etc (especially while injecting very strong current densities: see next section). The gradient of temperature between the top and bottom of the membrane is about one degree, and is well controlled by measuring the thermoelectric power [18].

It is important to note that the temperature of the membrane is kept constant (slightly above room temperature), in order to avoid magnetostrictive effects due to the thermal expansion of the polycarbonate membrane. For this reason, an external (macroscopic) thermostat cannot be used in these experiments.

During the AC temperature excitation, a current is injected in the wires in order to measure the magnetoresistance. The current injected at a first stage of the study is weak, typically of the order of $20 \mu A$ (about $2 \cdot 10^5 A/cm^2$), and has no effects in terms of spin-transfer. The signal is analyzed numerically (using Labview program) with the following expression:

$$V(t) = a0 + a1 \cos(2\pi ft + a2) + a3 \cos^2(2\pi ft + a4) \quad (4)$$

where:

- $a0$: $R_{AMR} = \frac{a0}{I}(H)$ is the magnetoresistance.

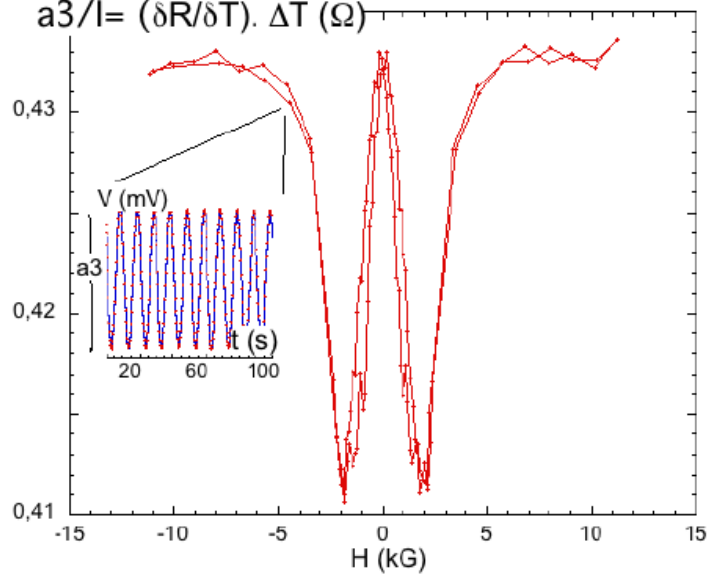


FIG. 3: Thermal susceptibility of the magnetoresistance as a function of the magnetic field. The angle of the applied field is about 80° , the current density is 0.2 MA/cm^2 , and the amplitude of the temperature variation is $\Delta T \approx 3 \text{ K}$ (around $T_0 = 300 \text{ K}$). Inset: the parameter $a3/I$ is the amplitude of the voltage response to a sinusoidal temperature variation obtained by the fit (blue line).

- **$a1$** : correction due to the induction produced by the heater.
- **$a3 = \frac{\Delta V}{\Delta T} \cdot \Delta T$** : amplitude of the response to the thermal excitation, or "thermal susceptibility of the magnetoresistance" (this term will be justified below).
- **$a2, a4$** : phase corrections.

The corresponding fit is plotted in the left inset of Fig. 3. As will be described below, the main contribution of the signal (plotted as a function of the time in the inset) is due to the temperature dependence of the resistance $R(T)$. The contribution of interest is the *spin-dependent contribution* of this signal that can be extracted from the fit (through the coefficient $a3$) and plotted as a function of the magnetic field H (Fig. 3). The profile obtained is typical for all measured samples (see also results and discussions in [17, 28, 29] for systems exhibiting GMR).

Figure 4 shows the profiles of the coefficient $a3/I(H)$ for different values of the angle of

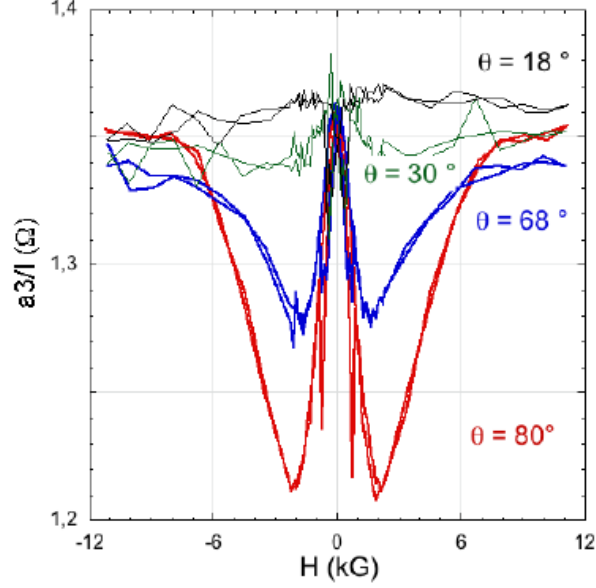


FIG. 4: Magnetic susceptibility of the magnetoresistance as a function of the magnetic field for different angles of the applied field.

the applied field. The signal is anisotropic so that this contribution is clearly due to a bulk effect. Interface effects (like those measured with the thermoelectric power on equivalent samples [18]) are not observed at small current densities. The irreversible jump of the magnetization, observed in the AMR curve (Fig. 1) can also be seen in the $a3/I(H)$ profile. However, we focus here on the reversible branches of the hysteresis. In the following, the angle of the applied field will be fixed around 80° because the signal is large and spin-transfer is maximal [12, 14].

How can we analyze this signal? Due to the high aspect ratio, the current density is perfectly uniform inside the wire (except at the interface with the contacts), and from that point of view, the metallic wire is one-dimensional. Defining the wire axis by the coordinate z , the kinetic equations writes (for our galvanostatic experiments the current density is constant).

$$\begin{cases} J_e = -\frac{\sigma}{|e|} \frac{\partial \mu}{\partial z} + \mathcal{S} \sigma \frac{\partial T}{\partial z} \\ J_Q = -|e| \mathcal{S} T J_e - \kappa \frac{\partial T}{\partial z} \end{cases} \quad (5)$$

with the electronic charge e and where μ is the electrochemical potential ($\frac{dV}{dz} = -\frac{1}{|e|} \frac{\partial \mu}{\partial z}$

is the electric field), J_e electric current, and J_Q the heat current. The corresponding transport coefficients are the conductivity σ and Fourier coefficient κ . The Onsager cross-coefficient are described by the Seebeck coefficient \mathcal{S} (or the Peltier coefficient $T\mathcal{S}$). Using the Wiedemann-Franz law $\kappa = \mathcal{L}_0\sigma T$, we introduce the Lorentz constant \mathcal{L}_O . Eq. (5) rewrites:

$$\frac{\partial\mu}{\partial z} = -|e|\rho(H, T) \left(1 + \frac{|e|\mathcal{S}^2(T)}{\mathcal{L}_0} \right) J_e - \frac{|e|\mathcal{S}(T)}{\mathcal{L}_0 T} \rho(H, T) J_Q \quad (6)$$

where the conductivity $\rho = 1/\sigma$, function of the magnetization states M and the temperature T , has been introduced.

The ratio $\mathcal{S}^2/\mathcal{L}_0 \approx 0.01$ is small for Ni and can be neglected in the first term on the right hand side of Eq. (6). On the other hand, the second term in the right hand side corresponds to the voltage when no current passes through the wire and gives the thermoelectric power (TEP). This term has been studied in details in a previous work [18]. It is here given by the voltage measured at zero current, i.e. by the term $a3(I = 0)$ according to Eq. (4) (in the following, the coefficient $a3$ will be corrected by the thermoelectric effect $a3(I) \leftarrow a3(I) - a3(I = 0)$). With this correction Eq. (6) simply reduces the Ohm's law: $\frac{dV}{dz} = \rho(H, T)J_e$. Integrating over the wire of length l , we have

$$V(H, T) = \rho(H, T) \frac{l}{A} I \quad (7)$$

where I is the current flowing in the section A of the wire. The validity of this expression can be check by measuring the coefficient $a3(I)$ as a function of the current (see Fig. 5). The TEP, i.e. the coefficient $a3(I = 0)$, is shown in the inset with the magnification around $I = 0$. At very large I (which is the region of interest for the study of spin-transfer) the deviation observed in Fig. 5 is mainly due to the Joule effect that modifies the temperature of the sample. The discussion related to spin-transfer effect is postpone for the next section.

The coefficient $a3$ measurement is defined by the thermal variation of the voltage. In terms of resistance we have:

$$\frac{a3}{I} = \frac{\partial R_{AMR}}{\partial T} \Delta T = \left(\frac{l\Delta T}{A} \right) \frac{\partial \rho}{\partial T} \quad (8)$$

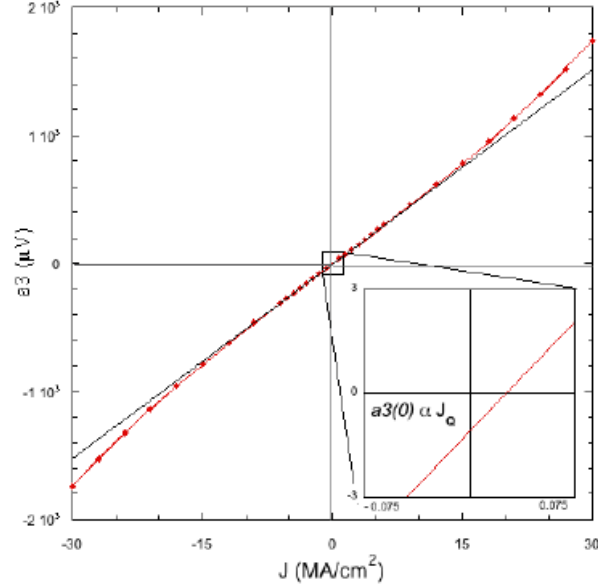


FIG. 5: Thermal susceptibility of the magnetoresistance as a function of the current injected into the wire at $H = 0$. The magnification around $I = 0$ shows the contribution of the TEP

Introducing the expression of the AMR Eq(1)

$$\frac{\partial \rho(H, T)}{\partial T} = \frac{\partial \rho_{\perp}(T)}{\partial T} + \frac{\partial \Delta \rho(T)}{\partial T} \left[\frac{M(H, T)}{M_s} \right]^2 + 2\Delta \rho(T) \left[\frac{M(H, T)}{M_s} \right] \underbrace{\frac{1}{M_s} \frac{\partial M}{\partial T}}_{\chi_T} \quad (9)$$

where the last term defines the thermal susceptibility of the magnetization $\chi_T = \frac{1}{M_s} \frac{\partial M}{\partial T}$. In the temperature range of the experiment [290K, 310K], the temperature variation of the AMR is very small, and the second term in the right hand side is neglected. Inserting Eq. (1) we obtain the thermal susceptibility as a function of the measured parameters :

$$\chi_T(H) = \frac{\partial \tilde{\rho}(H, T)}{\partial T} \frac{1}{2\Delta \rho(T)} \sqrt{\frac{\Delta \rho}{\tilde{\rho}(H, T)}} \quad (10)$$

Where $\tilde{\rho}(H, T) = \rho(H, T) - \rho_{\perp}(T)$, and $\frac{\partial \rho}{\partial T}$ is field independent and constant within our temperature range. In conclusion, since both the temperature variation of the resistance and the magnetoresistance hysteresis loops $\rho(H, T)$ are known, the protocol described here allows the ferromagnetic thermal susceptibility of a single nanowire to be measured.

It should be noticed that the $a3$ profiles (Fig. 3, Fig. 4) are rather similar to that of the derivative $\frac{\partial \rho}{\partial H}$ of the AMR profile, i.e. the field susceptibility $\chi_H = \frac{1}{M_s} \frac{\partial M}{\partial H}$. This is due to

a general property: both susceptibilities are proportional to the static fluctuations. In our case, $M = M_s \langle \cos(\varphi) \rangle$ is the equilibrium mean value of the magnetization (projected over the wire axis). We have $M = 2\pi M_s \int_0^\pi \cos(\varphi) e^{-V(H,\varphi)/kT} \sin\varphi d\varphi / Z$, where $Z(H, T)$ is the partition function and $V(\vec{H}, \varphi)$ is composed by an anisotropy term $K \sin^2(\varphi)$ and the Zeeman term $-\vec{M} \cdot \vec{H}$ (Eq. (2)).

The thermal susceptibility writes:

$$\begin{aligned} \chi_T = & -\frac{HM_s}{kT^2} (\langle \cos(\varphi) \cos(\theta - \varphi) \rangle - \langle \cos(\varphi) \rangle \langle \cos(\theta - \varphi) \rangle) \\ & + \frac{K}{kT^2} (\langle \cos(\varphi) \sin^2(\varphi) \rangle - \langle \sin^2\varphi \rangle \langle \cos(\varphi) \rangle) \end{aligned} \quad (11)$$

On the other hand, the field susceptibility writes:

$$\chi_H = \frac{M_s}{kT} (\langle \cos(\varphi) \cos(\theta - \varphi) \rangle - \langle \cos(\varphi) \rangle \langle \cos(\theta - \varphi) \rangle) \quad (12)$$

The following relation between the susceptibilities is obtained:

$$\chi_T = -\frac{H}{T} \chi_H + \frac{K}{kT^2} (\langle \cos^3\varphi \rangle - \langle \cos^2\varphi \rangle \langle \cos\varphi \rangle) \quad (13)$$

It is hence possible to identify the contributions due to the field susceptibility (first term in the right hand side in Eq. (13), and the correction due to the fluctuations of higher order. In Fig. 6, both profiles are superimposed : the contribution $(H \cdot \chi_H / T)$ is deduced from the measured AMR (red dashed line) and $a3/I$ is measured with our protocol. The deviation is due to the contribution of the fluctuations of higher order, that tends to reduce the apparent anisotropy (the minima are pushed toward zero). This observation will be useful in order to understand the effect of high current injection in the next section.

C. Ferromagnetic Entropy and spin-transfer

It has been shown that the spin-transfer effect occurs in these samples while injecting a DC current (or pulsed current) with a density of the order of 10^7 A/cm^2 [12, 14, 15]. The spin-transfer is evidenced by the shift of the switching field, i.e. the shift of the position of the irreversible jump, proportional to the current above a given threshold of the order of 10^7 A/cm^2 . A decrease of the switching field by a factor up to 50 % [15] has been observed. The after-effect measurements (or ferromagnetic relaxation) show that the effect

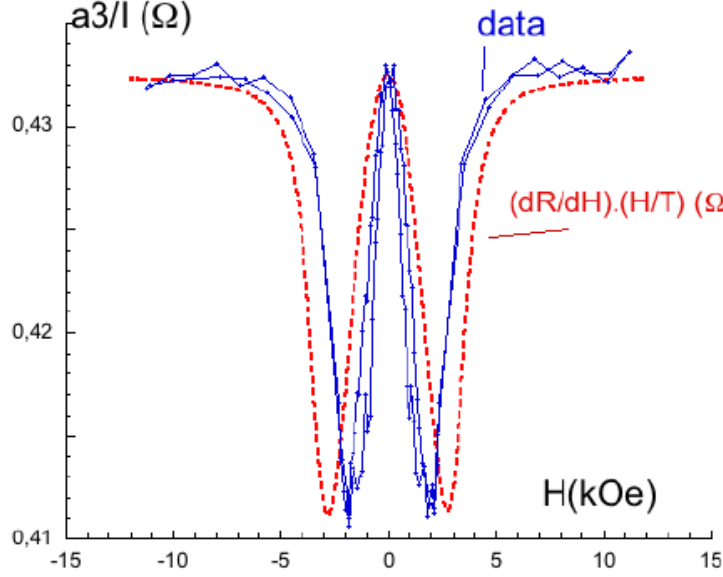


FIG. 6: Comparison between the thermal susceptibility (data) and the field susceptibility times H/T (dashed line) deduced. The deviation is due to the contribution of the moments of higher order (see text)

of the current injection induces an important modification of the parameters entering in the Néel-Brown activation law (related to the switching field). The effective potential barrier - or in stochastic terms the inverse of the effective temperature - decreases linearly as a function of the amplitude of the current. The effect is strong: 60 % variation is obtained between 1.5 and $4 \cdot 10^7 \text{ A/cm}^2$ (see fig. 4, first paper in Ref [13]). Meanwhile, the reversible part of the hysteresis loop is not significantly modified (see Fig. 7). Note that all these features are also observed in spin-valve structures [30, 31, 32]. These observations motivated the interpretation of a fully stochastic process generated by the kinetic coupling between the spin of conduction electron and the ferromagnetic order parameter (through the introduction of a relevant Onsager transport coefficient) [22].

In this context, the measurements of entropy at equilibrium (quasi-static states) allows the contribution of ferromagnetic fluctuations to be quantified and compared to the deterministic contribution in terms of rotation of the magnetization, as performed below.

Fig. 7 shows three hysteresis loops normalized to R_{max} , with currents density 0.2 MA/cm^2 , 20 MA/cm^2 and 40 MA/cm^2 : the three profiles seem to be superimposed except

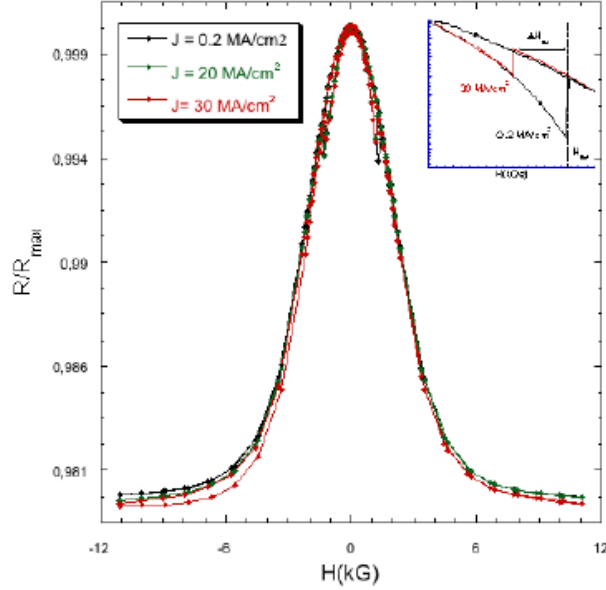


FIG. 7: Comparison between AMR Hysteresis loops of reference, and under high current injection. The reversible part of the hysteresis is not significantly affected by spin-transfer. Inset: zoom of the irreversible part with the two switching fields

for the position of the switching field (not shown here: see [12, 13, 14, 15] for the study of the irreversible jumps). The signal corresponding to the rotation of the magnetization, if any, is too small to be extracted from the noise in Fig. 7.

On the other hand, Fig. 8 shows that the thermal susceptibility $a_3/I(H)$ as a function of the magnetic field is significantly modified by injecting high currents. Since the contribution due to the Joule effect does not depends on the magnetic field, the variation observed is due to the magnetic susceptibility. Fig. 8(a) shows that the field dependence of the thermal susceptibility is significantly modified. Fig. 7 (b) compares the thermal susceptibility of the magnetoresistance for a weak current (reference current 0.2 MA/cm^2) and a strong current (45 MA/cm^2). The difference is due to the current injection. In the inset, the comparison is performed with the two corresponding ferromagnetic susceptibility deduced from Eq. (10).

According to the following Maxwell equation (see e.g. the discussion developed in the context of magnetocaloric effect [23, 33]),

$$\delta S = \int_{-H_{sat}}^{H_{sat}} \left(\frac{\partial M}{\partial T} \right)_H dH \quad (14)$$

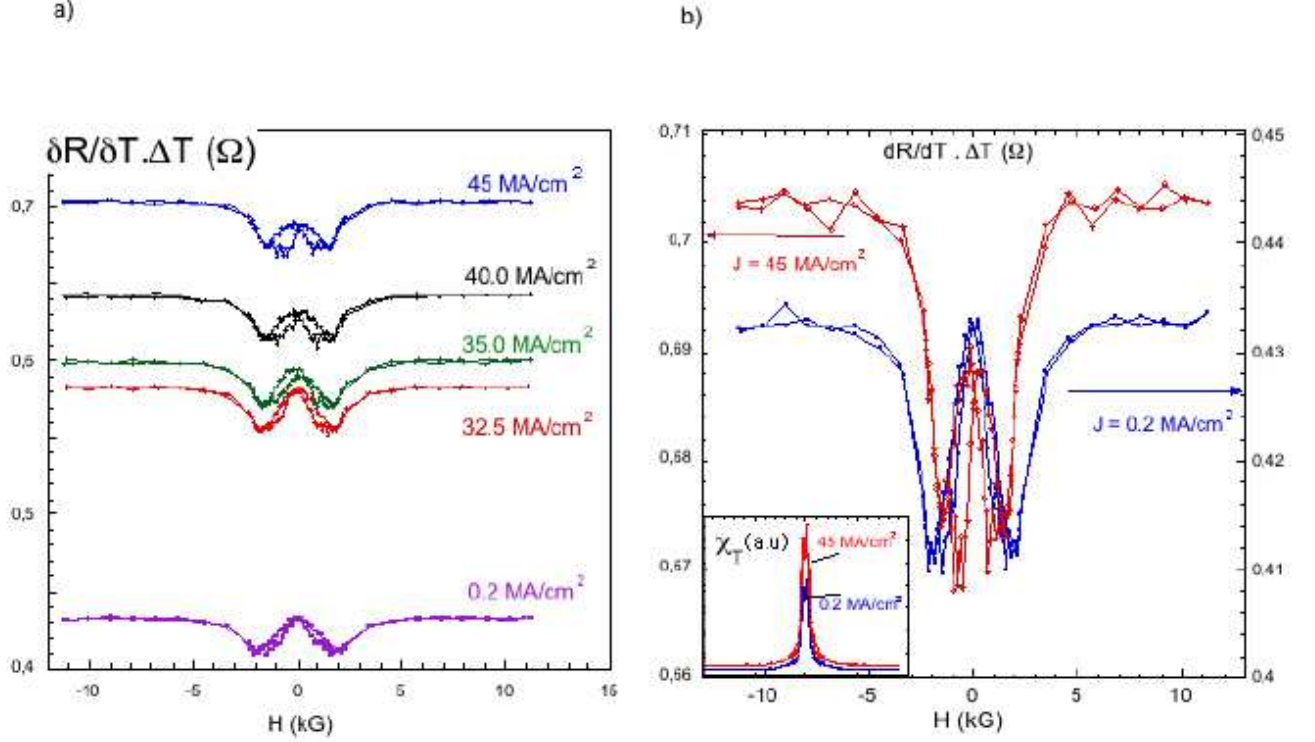


FIG. 8: (a) Thermal susceptibility of the magnetoresistance (coefficient a_3/I) as a function of the magnetic field for different current densities. (b) Comparison of the measurements with reference currents $J_0 = 0.2 \text{ MA/cm}^2$ and at high current $J = 45 \text{ MA/cm}^2$. Inset: corresponding magnetic susceptibilities (deduced from Eq. (10) and the measured AMR), some scale for the magnetic field

and recalling that the ferromagnetic system is at equilibrium (only the reversible branches of the hysteresis are investigated), the entropy variation due to the high current injection can be deduced from the measurements of the thermal susceptibility, presented in Fig. 8. We will take as a reference for the entropy of the ferromagnetic layer the integral of the susceptibility measured at 0.2 MA/cm^2 in the field range ± 1 Tesla: $S_{ref} \approx 8 \cdot 10^{-5} \text{ JK}^{-1} \text{ kg}^{-1}$ (using for Ni magnetization $M_s = 580 \cdot 10^{-3} \text{ J/Tcm}^3$ and for Ni density 8.9 g/cm^3).

In order to study the entropy generated by spin-transfer, i.e. for high current density, the entropy production is taken from the reference current density $J_0 = 0.2 \text{ MA/cm}^2$ ($I_0 = 0.02 \text{ mA}$):

$$\Delta S_{ST}(J) = \int_{-H_{sat}}^{H_{sat}} \left(\frac{\partial M}{\partial T}(J) - \frac{\partial M}{\partial T}(J_0) \right) dH \quad (15)$$

The result $\Delta S/S_{ref}$ is plotted in Fig. 8. The magnetic field induced by the current has

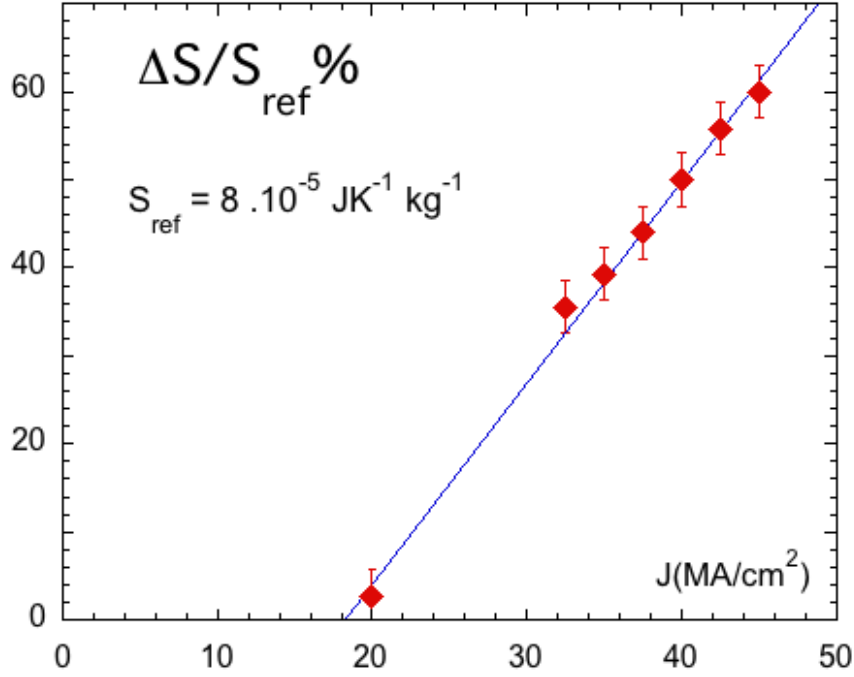


FIG. 9: Ferromagnetic entropy production due to current injection as a function of the current density. The entropy is calculated in the field range $\pm H_{sat} = \pm 1T$. The error bars account for the field induced by the current and Joule heating.

been taken into account in the error bars as follow: the induced field (about $\pm 5 \cdot 10^{-3} T/mA$, see discussion in [14]) is taking into account with a homogeneous field of ± 0.1 Tesla added to the integration interval. The variation is linear with the current and reaches 60 % at $4.5 \cdot 10^7 A/cm^2$. A current threshold is clearly visible and is of the order of $2 \cdot 10^7 A/cm^2$. All those characteristics are quantitatively and qualitatively that measured for spin-transfer experiments in Ni nanowires based on activation processes on the irreversible jumps.

Furthermore, the analysis of the variations due to current injection (Fig. 8 (b)) shows that the spin-transfer reduces the apparent anisotropy (i.e. the position of the minima peaks). The main contribution is hence apparently due to the fluctuations related to the moments of high orders (of the type $\langle \cos^3(\varphi) \rangle$ or $\langle \cos^2(\varphi) \rangle \langle \cos(\varphi) \rangle$). This problem, namely the identification of the specific form of the fluctuations, will be investigated in more detail elsewhere.

D. Conclusion

An experimental protocol has been described that allows the effect of a high DC current injected in a ferromagnetic nanowire to be investigated on the reversible branches of the hysteresis loop. The protocol is based on the measurements of the thermal magnetic susceptibility through the magnetoresistance properties and allows the ferromagnetic fluctuations and the entropy generated by spin-injections at high current densities to be deduced.

The results show a giant linear increase of the ferromagnetic entropy with the current injection: up to 60 % at $4.5 \cdot 10^7 \text{ A/cm}^2$. A clear current threshold is also present at about $2 \cdot 10^7 \text{ A/cm}^2$. These characteristics are exactly that previously measured on the irreversible part of the hysteresis in the case of experimental protocols based on the activation process (e.g. effective energy barrier, measure of critical current at given magnetic field, or measure of the shift of the switching field as a function of the current). Consequently, we attribute the observed increase of entropy measured as a function of the current (Fig. 9) to spin-transfer effect.

Furthermore, the effect of current injection on the equilibrium (quasi-static) states of the magnetization shows that the spin-transfer generates strong fluctuations of the magnetization (or incoherent excitations), instead of rotation of the magnetization or coherent spin-waves (as does the external magnetic torque). Unfortunately, at this stage of the study, it is not possible to definitively answer to the question of whether the spin-transfer is fully stochastic (diffusion term in the dynamic equation) or if it can be described by a deterministic term in the dynamical equation. However, in the last case, the study shows that the effect of the deterministic torque generates fluctuations (incoherent excitations), and not coherent rotation or coherent spin-waves.

On the other hand, it has been also observed that the most important contribution of the fluctuations seem to be generated by statistical moments of higher order, beyond the second moment. A more detailed analysis is hence necessary in order to understand the specificity of the excitations produced by the spin-transfer, and to be able to answer the above question about the stochasticity, in the framework of the thermodynamic approach reported here.

E. Acknowledgement

We thank L. C. Sampaio, Renato A Silva, and A. P. Guimarães for useful discussions and comments.

-
- [1] M. Tsoi et al. Phys. Rev. Lett. **80**, 4281 (1998); J-E. Wegrowe et al. Europhysics lett. **45** 626 (1999); F. J. Albert et al. Appl. Phys. Lett. **77** 3809 (2000); J. Grollier et al. Appl. Phys. Lett. **78**, 3663 (2001); E. B. Myers et al. Phys. Rev. Lett. **89**, 196801 (2002); J. Z. Sun et al. Appl. Phys. Lett. **81**, 2202 (2002); J.-E. Wegrowe et al. Appl. Phys. Lett. **80**, 3775 (2002); B. Oezylmaz et al. Phys. Rev. Lett **91**, 067203 (2003).
 - [2] L. Berger, Phys. Rev. B **54**, 9353 (1996).
 - [3] J. Slonczewski, J. Magn. Magn. Mat, **159** L1 (1996)
 - [4] J.-E. Wegrowe, M. C. Ciornei, H.-J. Drouhin, J. Phys.: Condens. Matter **19**, 165213 (2007).
 - [5] C. Serpico, I. D. Mayergoyz, G. Bertotti, M. D'Aquino, R. Bonin, Physica B **403**, 282 (2008).
 - [6] Fukushima et al. J. Appl. Phys. **99**, 08H706 (2006), Fukushima et al. IEEE Trans-Mag **41** 2571 (2005).
 - [7] P. Weiss, A. Piccard C. R. Acad. Sci. (Paris) **166** (1918) 352, P. Weiss, R. Forrer, C. R. Acad. Sci., **178** (1924) 1347.
 - [8] W. Wernsdorfer et al Phys. Rev. Lett. **77** (1996), 1873.
 - [9] J. -E. Wegrowe, D. Kelly, A. Franck, S. Gilbert, J.-Ph. Ansermet, Phys. Rev. Lett. **82** (1999), 3681.
 - [10] Y. Jaccard, Ph. Guittienne, D. Kelly, J.-E. Wegrowe, J-Ph. Ansermet,, Phy. Rev. B, **62** (2000), 1141.
 - [11] A. Fert, L. Piraux J. Magn. Magn. Mat. **200** 338 (1999).
 - [12] J-E. Wegrowe, D. Kelly, Y. Jaccard, Ph. Guittienne, and J.-Ph. Ansermet Europhysics lett. **45** 626 (1999), J.-E. Wegrowe, D. Kelly, T. Truong, Ph. Guittienne, J.-Ph. Ansermet, Europhysics lett. **56**, 748 (2001).
 - [13] Ph. Guittienne, J.-E. Wegrowe, D. Kelly, and J.-Ph. Ansermet, IEEE Trans. Mag. Magn-**37**, 2126 (2001), Ph. Guittienne, L. Gravier, J.-E. Wegrowe, and J.-Ph Ansermet J. Appl. Phys. **92**, 2743 (2002), J.-E. Wegrowe, X. Hoffer, Ph. Guittienne, A. Fabian, L. Gravier, T. Wade,

- J-Ph. Ansermet, J. Appl. Phys **91** , 6806 (2002).
- [14] D. Kelly, J. -E. Wegrowe, Trong-kha Truong, X. Hoffer, Ph. Guittienne, and J. -Ph. Ansermet, Phys. Rev. B **68** 134425 (2003).
- [15] J. -E. Wegrowe, M. Dubey, T. Wade, H. -J. Drouhin, and M. Konczykowski, J. Appl. Phys. **96** 4490 (2004).
- [16] L. Gravier, J. -E. Wegrowe, T. Wade, A. Fabian, and J. -Ph. Ansermet, IEEE Trans. Mag. Mat. **38**, 2700 (2002), L. Gravier, A. Fabian, A. Rudolf, A. Cachin, J. -E. Wegrowe, and J. -Ph. Ansermet, J. Magn. Magn. Mater. **271**,153 (2004), L. Gravier, S. Serrano-Guisan, and J. -Ph. Ansermet, J. Appl. Phys. **97**, 10C501 (2005), L. Gravier, S. Sarrano-Guisan, F. Reuse, and J.-Ph. Ansermet, Phys. Rev. B, **73**, 052410 (2006).
- [17] S. Serrano-Guisan, L. Gravier, M. Abid, and J. -Ph. Ansermet, J. Appl. Phys. **99**, 08T108 (2006).
- [18] J.-E. Wegrowe, Q. Anh Nguyen, M. Al-Barki, J.-F. Dayen, T. L. Wade, and H.-J. Drouhin, Phys. Rev. B **73** 134422, (2006).
- [19] E. Shapira, A. Tsukernik, and Y. Selzer, Nanotechnology **18**, 485703 (2007).
- [20] E. B. Myers et al. Science **285**, 867 (1999)
- [21] T. Y. Chen, Y. Ji, M. D. Stiles and C. L. Chien, Phys. Rev. Lett. **93**, 026601 (2004).
- [22] J.E. Wegrowe, S. M. Santos, M.-C. Ciornei, H.-J. Drouhin, M. Rubi., Phys. Rev. B **77**, 174408 (2008)
- [23] V. Basso, G. Bertotti, M. LoBue, C.P. Sasso, J. Magn. Magn. Mat. **290** (2005) 651.
- [24] J. -E. Wegrowe, S. Gilbert, D. Kelly, B. Doudin J.-Ph. Ansermet IEEE Trans. Magn. **MAG.-34** (1998), 903.
- [25] T. Wade, J.-E. Wegrowe, Eur. Phys. J. Appl. Phys. **29**, 3-22 (2005).
- [26] T. R. McGuire and R. I. Potter, IEEE Trans. vol **MAG-11**, 1018 (1975).
- [27] W. F. Brown Jr., *Micromagnetics*, Interscience publishers, 1963.
- [28] S. Serrano-Guisan, G. DiDomenicantonio, M. Abid, J.-P. Abid, M. Hillenkamp, L. Gravier, J.-Ph. Ansermet, and Ch. Felix, Nature Mater **5**, 730 (2006),
- [29] E. E. Fullerton and S. Mangin, Nature Mat. **7** (2008).
- [30] J.-E. Wegrowe, Phys. Rev. B **68**, 214414 (2003).
- [31] S. Urazhdin, O. Norman, W. Birge, W. P. Pratt, and J. Bass, Phys. Rev. Lett. **92**, 146803 (2003); S. Urazhdin, H. Kurt, W. P. Pratt, and J. Bass, Appl. Phys. Lett. **83**, 114 (2003).

- [32] A. Fabian, C. Terrier, S. Serrano Guisan, X. Hoffer, M. Dubey, L. Gravier, J.-Ph. Ansermet, and J.-E. Wegrowe, Phys. Rev. Lett. **91**, 257209 (2003).
- [33] V. K. Pecharsky and K.A. Gschneidner, Phys. Rev. Lett. **78** 4494 (1997), A. guiguière et al. Phys. Rev. Lett **83**, 2262 (1999), K. A. Gschneidner et al. Phys. Rev. Lett. **85**, 4190 (2000), J. R. Sun et al., Phys. Rev. Lett. **85**, 4191 (2000), F. Casanova et al. Phys. Rev. B **66**, 100401 (2002)
- [34] P. Podar, J. Gass, D. J. Rebar, S. Srinath, H. Srikanth, S. A. Morison, E. E. Carpenter, J. Magn. Magn. Mat. **307**, 227, S. Hariharan and J. Gass, Rev. Adv. Mater. Sci. **10** (2005) 398
- [35] V. Franco, K. R. Pirota, V. M. Prida, A. M. J. C. Neto, A. Conde, M. Knobel, B. Hernando, and M. Vazquez, Phys. Rev. B **77**, 104434 (2008).